Volatility of Ammonium Chloride over Aqueous Solutions to High Temperatures

Donald A. Palmer* and John M. Simonson

Chemistry Division, Oak Ridge National Laboratory, P.O. Box 2008, Oak Ridge, Tennessee 37831-6110

The partitioning of ammonium chloride from aqueous solutions to the vapor phase was measured from 120 to 350 °C. The experiments were performed in a platinum-lined autoclave from which samples of the liquid and vapor phases were withdrawn for analysis by ion chromatography, and acidimetric titration. The liquid-phase pH was maintained either with an excess of hydrochloric acid or by excess ammonia in the ammonium chloride solutions. The molal thermodynamic partitioning constants for NH_4Cl were calculated from the observed liquid- and vapor-phase concentrations, taking into account the known partitioning coefficients of HCl and NH_3, as well as the known mean stoichiometric activity coefficients of the ionic species in the liquid phase. The partitioning constants for NH_4Cl, NH_3, and HCl are represented as simple functions of temperature and water density. Some discussion is given of the relevance of these results to modeling the transport of chloride in power plants using ammonia to control the pH of the water/steam cycle.

Introduction

The results of monitoring (*1*) the chemical carryover of chloride in the water/steam cycles of power plants have been correlated with the expected ammonium chloride volatility in those plants using all-volatile treatment (AVT). It was found (1, 2) that chloride levels observed in the high-temperature steam are significantly higher than predicted on the basis of solute volatility ratios, commonly referred to as ray diagrams (*3*). Thus, a quantitative assessment of the total vapor-phase chloride concentration in equilibrium with ammonium chloride solutions is essential to the interpretation and prediction of power-plant operations based on AVT.

The equilibria involved in the liquid-phase aqueous chemistry of ammonium chloride are summarized as follows:

$$NH_4^+(aq) \rightleftharpoons NH_3(aq) + H^+(aq) \quad (1)$$

$$NH_3(aq) + H_2O \rightleftharpoons NH_4^+(aq) + OH^-(aq) \quad (2)$$

$$NH_4^+(aq) + Cl^-(aq) \rightleftharpoons NH_4Cl(aq) \quad (3)$$

$$H^+(aq) + Cl^-(aq) \rightleftharpoons HCl(aq) \quad (4)$$

Equations 1 and 2 are related through the ionization of water (*4*):

$$H_2O \rightleftharpoons H^+(aq) + OH^-(aq) \quad (5)$$

The solutes are assumed to partition to the vapor phase as neutral species, such that the partitioning equilibria are represented by

$$NH_3(aq) \rightleftharpoons NH_3(vap) \quad (6)$$

$$HCl(aq) \rightleftharpoons HCl(vap) \quad (7)$$

$$NH_4Cl(aq) \rightleftharpoons NH_4Cl(vap) \quad (8)$$

The thermodynamic properties at high temperatures of the reactions needed to interpret the chemistry of the ammonium chloride system are known from previous studies. Conductance (*5*) and electromotive force (emf) (*6*) studies provided the thermodynamic equilibrium constants for reactions 1 and 2. Ammonium chloride activity coefficients are available from Theissen and Simonson (*7*). Models for the activity coefficients of HCl(aq) based on experimental results at high temperatures were reported by Holmes et al. (*8*) and Simonson et al. (*9*). The partitioning of ammonia between liquid and vapor phases, eq 6, was studied to high temperatures (*10, 11*). The volatility of aqueous HCl was measured recently by Simonson and Palmer (*12*) from 50 to 350 °C using an apparatus similar to that used in the present study.

The overall reactions are combinations of eq 3 with eq 8 and eq 4 with eq 7:

$$NH_4^+(aq) + Cl^-(aq) \rightleftharpoons NH_4Cl(vap) \quad (9)$$

$$H^+(aq) + Cl^-(aq) \rightleftharpoons HCl(vap) \quad (10)$$

Reactions 9 and 10 are responsible for the transport of chloride ion from aqueous ammonium chloride solutions. Therefore, their relative importance in the observed partitioning of chloride from aqueous ammonium chloride solutions depends on the magnitudes of the individual thermodynamic partitioning coefficients for reactions 9 and 10 and on the pH of the aqueous solution. As the partitioning constants for hydrochloric acid are also known (*12*), only the thermodynamics of reaction 9 are needed for a complete description of the partitioning of chloride from aqueous ammonium chloride solutions at high temperatures.

Two sets of experimental conditions were investigated in the present study. The pH of the solution was buffered either by a mixture of ammonium chloride and ammonia or by an excess of hydrochloric acid. Partitioning coefficients for NH_4Cl were calculated from the observed excess chloride and nitrogen levels in both sets of experiments. The pH of the liquid was determined by titration of the free ammonia in the case of the ammonia/ammonium buffered experiments and by titration of the free protons in the acidic solutions; the pH at experimental temperatures was then calculated directly from the known ionization properties of ammonia (*5, 6*) and water (*4*). In those condensed vapor samples where the concentration of HCl was sufficiently high, the acidity was also measured directly by acidimetric titration. Note that in the present study, pH is defined as the negative logarithm of the hydrogen ion molality.

Experimental Section

Equipment. The basic equipment was described previously (*12*), although significant modifications were made

* To whom correspondence should be addressed.

0021-9568/93/1738-0465$04.00/0

subsequently. A brief description of the modified apparatus is given here.

The platinum liner was contained in a stainless steel pressure vessel (*ca.* 900 cm^3 internal volume) seated in a Marshall tube furnace (±0.1 °C). In contrast to the earlier design (*12*), the liquid phase inside the liner was linked to a Teflon bag inside a water-filled, room-temperature autoclave open to the annular space around the platinum liner. Mass transfer between the two autoclaves served to equalize the pressure across the platinum liner. Pressures in both the annular space and liner were monitored with two pressure transducers. Two concentric platinum tubes gold-welded to the top of the liner passed through a compression fitting in the pressure vessel. The inner tube extended to the bottom of the liner and was used to sample the liquid phase, whereas vapor-phase samples were drawn through the annular space between the two tubes. Both liquid- and vapor-phase sample tubes (1/32-in. o.d.) extended out of the furnace, through water-cooled condensers, and were finally connected to PEEK (Upchurch Scientific) valves. A 1/8-in. platinum thermal well, which passed through a second compression fitting in the high-temperature autoclave, extended to near the bottom of the liner and was sealed to the liner by a gold weld. It contained a (0.06-in. o.d.) calibrated four-lead PRTD to monitor the temperature of the liquid phase within the liner. An additional heater was wrapped around the sample tubes where they exited the autoclave. This heater maintained the temperature slightly above that of the liquid phase in the liner, to prevent condensation and refluxing of vapor-phase samples in the sample tube.

Liquid-phase samples were collected directly in disposable syringes. Condensed vapor-phase samples were obtained at ambient temperature and the prevailing experimental pressure by using a third pressure vessel equipped with a collapsible Teflon bag. Water was withdrawn from this vessel with a positive-displacement pump at controlled rates, which were varied from 0.5 to 2.0 $cm^3 \cdot h^{-1}$ as a test for equilibrium. The mass of the partially water-filled Teflon bag was measured before and after sampling to determine the amount of condensed vapor collected.

The appropriate solution was purged with helium for at least 2 h to remove dissolved oxygen prior to injection into the platinum liner. Although these solutions were spiked with potassium chloride, no K^+ ion was detected in any of the vapor-phase cation analyses, indicating minimal aerosol carryover. Samples of the liquid phase were obtained immediately before and after a given vapor-phase sample was taken, and the average of the two analyses was assumed to be the liquid-phase composition corresponding to that vapor-phase sample. The concentrations of solutes in the liquid phase increased during a given sampling sequence due to preferential loss of water to the vapor phase. The observed molalities of the solutes in both phases are listed in Tables I and II.

Analytical Methods. The total ammonia and chloride concentrations in the liquid- and vapor-phase samples were measured by conventional ion chromatography, with the exception of those vapor-phase samples containing levels of total ammonia $<10^{-5}$ $mol \cdot kg^{-1}$, where the concentration method was used.

The acidities of the liquid samples were determined at 25 °C by titration using weight burets containing a standardized sodium hydroxide solution. The titration end points were corrected for the conversion of ammonium ion to ammonia at this pH. In those cases where the free proton or ammonia concentrations in the condensed vapor samples exceeded a minimum level of *ca.* 0.01 $mol \cdot kg^{-1}$, acidimetric titrations were performed to confirm the ion-chromatographic analyses.

Results and Discussion

Calculation of the values of the partitioning constant K_3 for NH_4Cl was based on the equilibrium equations

$$K_1 = \frac{m_v(NH_3)\gamma_v(NH_3)}{m_l(NH_3)\gamma_l(NH_3)} \quad (11)$$

$$K_2 = \frac{m_v(HCl)\gamma_v(HCl)}{m_l(H^+)m_l(Cl^-)\gamma_l(H^+)\gamma_l(Cl^-)} \quad (12)$$

$$K_3 = \frac{m_v(NH_4Cl)\gamma_v(NH_4Cl)}{m_l(NH_4^+)m_l(Cl^-)\gamma_l(NH_4^+)\gamma_l(Cl^-)} \quad (13)$$

$$K_H = \frac{K_W}{K_B} = \frac{m_l(H^+)\gamma_l(H^+)m_l(NH_3)\gamma_l(NH_3)}{m_l(NH_4^+)\gamma_l(NH_4^+)} \quad (14)$$

The subscripts l and v are used to refer to species in the liquid and vapor phases, respectively. The equilibrium constants K_1, K_2, K_3, K_H, K_B, and K_w correspond to the equilibria in eqs 6, 10, 9, 1, 2, and 5, respectively. It is assumed that all species in the vapor phase are completely associated (un-ionized). This assumption is supported from calculations based on the known relationships of ionization constants on the solvent density (*13, 14*). For example, taking the published equations for NaCl (*15*) and HCl (*16*) and the densities of water liquid and vapor (*17*) at 350 °C (ρ_l = 0.5747 $g \cdot cm^{-3}$, ρ_v = 0.1135 $g \cdot cm^{-3}$), the increase in the association constant for NaCl in the vapor phase compared to the liquid phase is 6.5 log units with a corresponding increase of 9.8 log units for HCl. These large differences in association constants in the two phases are consistent with the assumption of complete association of solute species in the vapor phase. It is further assumed that, at the relatively low solute molalities considered here, all uncharged species have unit activity coefficients.

Partitioning of ammonia at low molalities as represented by eq 6 has been reported to high temperatures by Jones (*10*) and Edwards et al. (*11*). These values may be represented accurately as a simple function (eq 15) of temperature and

$$\log K_1 = -0.056 + 458.71/(T/\mathrm{K}) + 1.3267 \log(\rho_l/(g \cdot cm^{-3})) \quad (15)$$

the density of the water in the liquid phase (ρ_l, $g \cdot cm^{-3}$) (*23*) as illustrated in Figure 1. It should be noted that the constraint of $\log K_1 = 0$ at the solvent critical condition was applied in determining the constants of eq 15.

Values of K_H were calculated from the international formulation for water substance ionization of Marshall and Franck (*4*) and from the equation for ammonia ionization given by Thiessen and Simonson (*7*):

$$\log K_H = a_H + \frac{b_H}{T/\mathrm{K}} + \frac{c_H}{(T/\mathrm{K})^2} + \frac{d_H}{(T/\mathrm{K})^3} + \left(e_H + \frac{f_H}{T/\mathrm{K}} + \frac{g_H}{(T/\mathrm{K})^2}\right) \log(\rho_l/(g \cdot cm^{-3})) \quad (16)$$

where a_H = 1.847, b_H = −5233.8, c_H = 9.3765 × 10^5, d_H = −1.0825 × 10^8, e_H = 11.767, f_H = −9488.8, and g_H = 8.5641 × 10^5.

Simonson and Palmer (*12*) expressed K_2 as a function of temperature and solvent density on the basis of their experimental results from 50 to 350 °C as well as existing literature values to 110 °C (*18, 19*):

$$\log K_2 = -13.4944 - 934.466/(T/\mathrm{K}) - 11.0029 \log(\rho_l/(g \cdot cm^{-3})) + 5.4847 \log(T/\mathrm{K}) \quad (17)$$

$\log K_2$ is shown in Figure 2 as a function of reciprocal

Table I. Liquid- and Vapor-Phase Compositions and Calculated Partitioning Constants K_3 for NH_4Cl (Measurements in Excess HCl)

liquid phase (averaged values)					vapor phase			K_3	
m_{Cl}/(mol·kg^{-1})	m_{NH_4}/(mol·kg^{-1})	m_H/(mol·kg^{-1})	$\gamma_\pm$(HCl)	$\gamma_\pm$(NH_4Cl)	m_{Cl}/(mol·kg^{-1})	m_N/(mol·kg^{-1})	m_H/(mol·kg^{-1})	as Cl	as NH_3
				t = 120 °C					
2.184	0.899	1.285	0.684	0.545	0.0812	3.02×10^{-7}		0.041	-3.5×10^{-7}
2.227	0.916	1.310	0.687	0.545	0.0423	3.84×10^{-6}		−0.030	5.7×10^{-6}
2.302	0.944	1.358	0.693	0.545	0.0748	3.39×10^{-7}		0.015	-2.4×10^{-7}
2.374	0.968	1.406	0.699	0.547	0.0773	2.22×10^{-7}		0.0096	-3.9×10^{-7}
2.484	1.025	1.459	0.706	0.547	0.0959	1.98×10^{-7}		0.024	-4.0×10^{-7}
2.577	1.060	1.517	0.714	0.549	0.0926	1.70×10^{-7}		0.0071	-3.7×10^{-7}
2.706	1.114	1.591	0.725	0.550	0.0928	2.71×10^{-7}		−0.0071	-2.3×10^{-7}
2.892	1.213	1.679	0.740	0.552	0.116	2.11×10^{-11}		5.3×10^{-4}	-4.6×10^{-7}
3.076	1.290	1.786	0.757	0.555	0.125	2.31×10^{-7}		−0.011	-1.9×10^{-7}
3.275	1.362	1.913	0.776	0.559	0.145	1.26×10^{-6}		−0.015	6.4×10^{-7}
				t = 150 °C					
1.146	0.769	0.280	0.559	0.495	0.005 57	3.08×10^{-5}		−0.035	1.1×10^{-4}
1.160	0.782	0.286	0.559	0.494	0.005 39	2.55×10^{-5}		−0.038	8.8×10^{-5}
1.200	0.804	0.294	0.559	0.492	0.006 33	9.70×10^{-6}		−0.036	1.5×10^{-5}
1.253	0.839	0.303	0.558	0.489	0.007 63	1.31×10^{-5}		−0.032	2.8×10^{-5}
1.289	0.874	0.312	0.557	0.487	0.014 5	2.47×10^{-5}		−0.0069	7.0×10^{-5}
1.323	0.908	0.322	0.557	0.486	0.008 49			−0.032	
1.374	0.949	0.333	0.557	0.483	0.008 67			−0.034	
1.422	1.004	0.345	0.556	0.482	0.010 5			−0.030	
0.992	1.016	0.034	0.544	0.495	0.006 47	6.59×10^{-5}		0.021	-2.9×10^{-5}
1.018	1.051	0.036	0.543	0.493	0.001 40	8.90×10^{-5}		2.4×10^{-5}	6.5×10^{-5}
1.032	1.085	0.036	0.541	0.492	0.001 50	1.11×10^{-4}		2.7×10^{-4}	1.4×10^{-4}
1.041	1.132	0.037	0.540	0.492	0.001 55	1.02×10^{-4}		3.1×10^{-4}	9.6×10^{-5}
1.087	1.177	0.038	0.538	0.488	0.001 79	1.23×10^{-4}		7.3×10^{-4}	1.6×10^{-4}
1.146	1.223	0.039	0.537	0.484	0.001 73	1.12×10^{-4}		8.7×10^{-5}	1.2×10^{-4}
1.175	1.209	0.041	0.538	0.483	0.002 73	6.04×10^{-4}		0.0028	0.0017
1.221	1.249	0.042	0.538	0.480	0.002 32	5.15×10^{-4}		0.0011	0.0013
1.258	1.284	0.043	0.537	0.478	0.002 33	2.58×10^{-4}		7.6×10^{-4}	5.2×10^{-4}
1.284	1.319	0.044	0.537	0.477	0.002 10	1.84×10^{-4}		-1.1×10^{-4}	3.0×10^{-4}
1.324	1.367	0.046	0.536	0.474	0.002 53	2.65×10^{-4}		6.7×10^{-4}	4.9×10^{-4}
1.373	1.428	0.047	0.534	0.472	0.002 37	1.36×10^{-4}		-1.4×10^{-4}	1.6×10^{-4}
1.421	1.479	0.049	0.534	0.470	0.002 66	1.44×10^{-4}		1.5×10^{-4}	1.6×10^{-4}
1.464	1.526	0.050	0.533	0.468	0.002 69	1.01×10^{-4}		-1.2×10^{-4}	6.7×10^{-5}
1.540	1.596	0.053	0.533	0.465	0.003 02	1.71×10^{-4}		1.5×10^{-5}	2.0×10^{-4}
1.379	1.405	0.047	0.536	0.472	0.002 74	4.00×10^{-4}		8.0×10^{-4}	8.1×10^{-4}
1.425	1.497	0.048	0.533	0.469	0.002 56	1.12×10^{-4}		-5.0×10^{-6}	9.0×10^{-5}
1.479	1.558	0.050	0.532	0.467	0.002 79	1.30×10^{-4}		1.1×10^{-4}	1.2×10^{-4}
1.538	1.623	0.052	0.532	0.465	0.003 03	9.13×10^{-5}		1.5×10^{-4}	3.9×10^{-5}
1.631	1.685	0.054	0.533	0.461	0.003 28	1.06×10^{-4}		3.0×10^{-6}	6.5×10^{-5}
1.756	1.750	0.057	0.536	0.457	0.003 54	1.15×10^{-4}		-3.3×10^{-4}	7.9×10^{-5}
1.844	1.813	0.060	0.537	0.453	0.003 98	5.65×10^{-5}		-3.1×10^{-4}	-1.1×10^{-5}
1.931	1.913	0.064	0.537	0.450	0.004 69	9.48×10^{-5}		5.8×10^{-5}	4.6×10^{-5}
2.072	2.050	0.068	0.539	0.446	0.005 47	9.38×10^{-5}		1.8×10^{-4}	4.0×10^{-5}
2.277	2.251	0.073	0.542	0.442	0.005 72	7.00×10^{-5}		-7.8×10^{-4}	1.0×10^{-5}
2.514	2.508	0.080	0.545	0.437	0.007 49	9.85×10^{-5}		-3.5×10^{-4}	3.5×10^{-5}
				t = 200 °C					
1.013	1.003	0.0325	0.453	0.423	0.004 66	1.56×10^{-4}		−0.0038	-8.2×10^{-4}
1.048	1.012	0.0336	0.452	0.420	0.005 97	4.67×10^{-4}		0.0016	9.4×10^{-4}
1.091	1.065	0.0348	0.449	0.416	0.006 24	3.23×10^{-4}		0.0011	1.4×10^{-4}
1.149	1.140	0.0360	0.446	0.412	0.006 76	4.11×10^{-4}		0.0013	5.0×10^{-4}
1.200	1.178	0.0372	0.444	0.408	0.007 30	2.00×10^{-4}		0.0016	-4.4×10^{-4}
1.248	1.218	0.0386	0.442	0.405	0.007 84	4.15×10^{-4}		0.0018	4.8×10^{-4}
1.312	1.273	0.0404	0.439	0.402	0.008 82	7.79×10^{-4}		0.0029	0.0019
1.382	1.335	0.0423	0.437	0.398	0.009 40	6.54×10^{-4}		0.0022	0.0013
1.477	1.409	0.0442	0.434	0.392	0.009 73	3.64×10^{-4}		9.8×10^{-5}	2.3×10^{-4}
1.621	1.523	0.0470	0.431	0.385	0.011 3	5.09×10^{-4}		2.9×10^{-4}	6.5×10^{-4}
1.773	1.650	0.0494	0.428	0.379	0.013 4	4.00×10^{-4}		0.0019	2.7×10^{-4}
1.149	1.146	0.0264	0.445	0.412	0.004 72	1.06×10^{-4}		-1.0×10^{-4}	−0.0014
1.184	1.168	0.0270	0.444	0.410	0.005 35	7.90×10^{-4}		0.0017	0.0016
1.211	1.188	0.0277	0.443	0.408	0.005 58	8.87×10^{-4}		0.0017	0.0020
1.259	1.218	0.0284	0.441	0.405	0.005 44	8.60×10^{-6}		-1.6×10^{-4}	−0.0016
1.309	1.287	0.0293	0.438	0.401	0.006 70	0.00103		0.0034	0.0024
1.355	1.371	0.0303	0.436	0.398	0.006 92	6.35×10^{-4}		0.0027	7.4×10^{-4}
1.416	1.435	0.0313	0.433	0.395	0.006 46	5.30×10^{-5}		-3.3×10^{-4}	−0.0012
1.510	1.505	0.0325	0.431	0.390	0.007 23	8.18×10^{-5}		9.9×10^{-5}	−0.0011
1.606	1.577	0.0338	0.429	0.385	0.008 53	7.14×10^{-4}		0.0018	8.0×10^{-4}
1.656	1.652	0.0351	0.427	0.383	0.009 42	0.001 25		0.0027	0.0021
1.347	1.306	0.0281	0.438	0.399	0.005 20			−0.0019	
1.396	1.340	0.0289	0.436	0.396	0.006 43	9.88×10^{-4}		0.0013	0.0019
1.417	1.378	0.0298	0.435	0.395	0.006 24	4.59×10^{-4}		-2.1×10^{-4}	1.0×10^{-4}
1.451	1.407	0.0307	0.434	0.393	0.006 77	6.34×10^{-4}		4.4×10^{-4}	6.8×10^{-4}
1.495	1.454	0.0314	0.433	0.391	0.007 17	7.02×10^{-4}		8.1×10^{-4}	8.6×10^{-4}
1.557	1.523	0.0319	0.430	0.388	0.007 35	5.08×10^{-4}		2.5×10^{-4}	2.1×10^{-4}

Table I (Continued)

liquid phase (averaged values)					vapor phase			K_3	
m_{Cl}/(mol·kg^{-1})	m_{NH_4}/(mol·kg^{-1})	m_H/(mol·kg^{-1})	$\gamma_\pm$(HCl)	$\gamma_\pm$(NH_4Cl)	m_{Cl}/(mol·kg^{-1})	m_N/(mol·kg^{-1})	m_H/(mol·kg^{-1})	as Cl	as NH_3
				t = 200 °C					
1.612	1.587	0.0331	0.429	0.385	0.008 11	7.03×10^{-4}		9.9×10^{-4}	7.3×10^{-4}
1.663	1.641	0.0343	0.428	0.382	0.008 46	5.88×10^{-4}		6.1×10^{-4}	4.0×10^{-4}
1.726	1.693	0.0355	0.426	0.380	0.009 02	5.64×10^{-4}		5.6×10^{-4}	3.4×10^{-4}
				t = 250 °C					
1.401	1.398	0.0282	0.318	0.309	0.0201	4.71×10^{-4}		-1.1×10^{-4}	−0.0057
1.436	1.451	0.0286	0.316	0.306	0.0231	0.003 28		0.013	0.0091
1.481	1.497	0.0290	0.314	0.304	0.0231	0.002 48		0.0088	0.0046
1.555	1.541	0.0294	0.311	0.300	0.0240	0.002 42		0.0083	0.0040
1.615	1.591	0.0297	0.309	0.297	0.0251	0.002 40		0.0096	0.0036
1.672	1.645	0.0299	0.306	0.294	0.0259	0.002 62		0.0099	0.0042
1.753	1.719	0.0302	0.303	0.290	0.0256	0.002 28		0.0046	0.0024
1.829	1.799	0.0304	0.301	0.287	0.0266	0.002 99		0.0050	0.0047
1.933	1.911	0.0305	0.297	0.282	0.0282	0.002 80		0.0072	0.0035
				t = 300 °C					
0.711	0.687	0.0218	0.230	0.265	0.0385	0.004 16		0.12	0.034
0.731	0.713	0.0211	0.228	0.262	0.0387	0.004 34		0.14	0.033
0.760	0.755	0.0206	0.224	0.258	0.0348	0.004 61		0.14	0.030
0.791	0.801	0.0201	0.221	0.254	0.0383	0.004 91		0.14	0.028
0.828	0.841	0.0195	0.217	0.250	0.0383	0.005 87		0.15	0.042
0.891	0.889	0.0188	0.210	0.243	0.0375	0.005 62		0.14	0.024
0.968	0.941	0.0181	0.204	0.235	0.0376	0.006 39		0.15	0.029
1.051	1.006	0.0173	0.197	0.227	0.0363	0.006 61		0.13	0.019
1.124	1.104	0.0164	0.192	0.222	0.0375	0.007 81		0.16	0.023
				t = 325 °C					
0.0960	0.0842	0.0116	0.351	0.445	0.0410	0.027 6	0.0146	12	17
0.0956	0.0864	0.0116	0.353	0.446	0.0527	0.040 2	0.0150	19	24
0.0968	0.0881	0.0114	0.351	0.444	0.0358	0.020 9	0.0165	8.6	12
0.0990	0.0895	0.0113	0.348	0.441	0.0433	0.029 5	0.0164	13	17
0.1011	0.0915	0.0112	0.346	0.439	0.0402	0.023 2	0.0168	11	13
0.1028	0.0931	0.0111	0.343	0.436	0.0416	0.026 4	0.0163	11	14
0.1040	0.0948	0.0110	0.342	0.435	0.0463	0.031 8	0.0155	14	17
0.1056	0.0972	0.0109	0.340	0.433	0.0458	0.031 2	0.0154	13	16
0.1585	0.1334	0.0231	0.286	0.379	0.244	0.007 31	0.0385	76	2.4
0.1679	0.1448	0.0218	0.280	0.372	0.0521	0.008 99	0.0344	2.0	2.3
0.1746	0.1515	0.0211	0.276	0.368	0.0618	0.009 25	0.0320	5.4	2.5
0.1969	0.1764	0.0199	0.263	0.354	0.0709	0.010 2	0.0300	7.2	2.2
0.2421	0.2225	0.0185	0.242	0.330	0.116	0.012 9	0.0237	16	2.2
0.2935	0.2760	0.0202	0.221	0.307	0.0573	0.007 55	0.0274	1.7	0.72
0.3320	0.1509	0.0273	0.202	0.293	0.0330	0.011 0	0.0313	−2.9	1.2
				t = 350 °C					
0.0732	0.0687	0.006 19	0.189	0.386	0.0424	0.0333	0.009 13	38	39
0.0749	0.0733	0.005 97	0.188	0.382	0.0340	0.0233	0.010 7	24	22
0.0774	0.0761	0.005 54	0.185	0.378	0.0355	0.0254	0.010 1	26	23
0.0804	0.0791	0.005 35	0.182	0.374	0.0363	0.0276	0.008 74	26	23
0.0825	0.0812	0.005 19	0.180	0.370	0.0442	0.0363	0.007 88	34	31
0.0851	0.0847	0.005 01	0.177	0.367	0.0478	0.0405	0.007 32	38	34
0.0881	0.0874	0.004 90	0.174	0.362	0.0554	0.0500	0.005 37	42	40
0.0905	0.0876	0.004 69	0.171	0.359	0.0811	0.0730	0.008 11	69	63
0.1081	0.0956	0.013 8	0.156	0.333	0.105	0.0939	0.013 6	62	79
0.1091	0.0977	0.013 6	0.155	0.332	0.0680	0.0525	0.016 7	29	42
0.1107	0.1003	0.012 7	0.154	0.331	0.0788	0.0685	0.014 1	39	54
0.1135	0.1038	0.012 5	0.153	0.328	0.0808	0.0678	0.014 5	40	51
0.1166	0.1069	0.012 3	0.150	0.324	0.0813	0.0686	0.014 4	39	49
0.1170	0.1094	0.012 4	0.150	0.324	0.0863	0.0738	0.013 5	41	52
0.1204	0.1132	0.012 2	0.148	0.321	0.0618	0.0463	0.017 8	23	30
0.1248	0.1156	0.011 5	0.146	0.317	0.0880	0.0764	0.013 1	41	49
0.1261	0.1149	0.011 3	0.145	0.316	0.0920	0.0797	0.012 6	44	51
0.0558	0.0496	0.006 45	0.213	0.420	0.0560	0.0478	0.006 80	81	89
0.0550	0.0495	0.006 16	0.215	0.422	0.0553	0.0490	0.006 21	84	94
0.0552	0.0498	0.005 74	0.216	0.422	0.0559	0.0498	0.006 10	85	94
0.0549	0.0498	0.005 48	0.216	0.423	0.0555	0.0472	0.005 80	86	88
0.0549	0.0501	0.005 15	0.216	0.424	0.0449	0.0400	0.005 80	66	73
0.0561	0.0513	0.004 78	0.214	0.421	0.0254	0.0190	0.008 24	27	28
0.0561	0.0524	0.003 95	0.215	0.422	0.0265	0.0216	0.006 66	32	30
0.0574	0.0558	0.002 44	0.214	0.421	0.0418	0.0411	0.002 45	68	55
0.0614	0.0603	0.001 56	0.207	0.413	0.0242	0.0230	0.002 37	33	8.0

temperature in kelvin.

As mentioned previously, the activity coefficients shown in eqs 11–14 for the uncharged solute species NH_3, HCl, and NH_4Cl are assumed to equal unity in both liquid and vapor phases at all experimental conditions. The stoichiometric mean-ionic activity coefficients $\gamma_\pm$ can be substituted for the liquid-phase activity coefficients using the definitions

$$\gamma_\pm^2(\mathrm{HCl}) = \gamma_1(\mathrm{H^+})\gamma_1(\mathrm{Cl^-}) \qquad (18)$$

Table II. Liquid- and Vapor-Phase Compositions and Calculated Partitioning Constants K_3 for NH_4Cl (Measurements in Buffered NH_3 + NH_4^+ Solutions)

liquid phase (averaged values)					vapor phase		K_3	
m_{Cl}/(mol·kg^{-1})	m_N/(mol·kg^{-1})	m_{NH_3}/(mol·kg^{-1})	$\gamma_\pm$(HCl)	$\gamma_\pm$(NH_4Cl)	m_{Cl}/(mol·kg^{-1})	m_N/(mol·kg^{-1})	as Cl	as NH_3
				t = 200 °C				
1.082	1.195	0.1125	0.448	0.416	4.70×10^{-4}	0.288	0.0024	−2.4
1.121	1.233	0.1115	0.446	0.413	1.46×10^{-4}	0.267	6.8×10^{-4}	−2.3
1.160	1.247	0.0870	0.444	0.411	6.76×10^{-5}	0.234	2.9×10^{-4}	−1.6
1.170	1.263	0.0930	0.444	0.410		0.196		−1.8
1.179	1.293	0.1140	0.443	0.409		0.156		−2.7
1.230	1.335	0.1055	0.441	0.406	2.13×10^{-5}	0.133	7.6×10^{-5}	−2.4
1.291	1.377	0.0855	0.438	0.402	4.24×10^{-5}	0.0943	1.5×10^{-4}	−1.9
1.357	1.421	0.0640	0.436	0.398	1.65×10^{-5}	0.0875	3.8×10^{-5}	−1.2
				t = 250 °C				
0.8265	1.304	0.4627	0.360	0.356		2.43		1.8
0.8520	1.246	0.4216	0.358	0.354		2.23		1.8
0.8756	1.238	0.4000	0.355	0.351		2.06		0.96
0.9030	1.221	0.3624	0.353	0.348		1.88		1.1
0.9302	1.227	0.3236	0.350	0.345	2.32×10^{-5}	1.67	1.2×10^{-4}	0.80
0.9519	1.237	0.2874	0.348	0.343	2.84×10^{-5}	1.50	1.5×10^{-4}	0.81
0.9814	1.224	0.2568	0.345	0.340	5.38×10^{-5}	1.35	3.6×10^{-4}	0.80
1.0085	1.238	0.2277	0.343	0.337	3.38×10^{-5}	1.20	1.5×10^{-4}	0.70
1.0395	1.279	0.1995	0.341	0.334	2.87×10^{-5}	1.05	7.2×10^{-5}	0.57
				t = 300 °C				
0.7101	1.127	0.4067	0.230	0.265	0.0713	1.43	2.1	−0.36
0.7397	1.119	0.3861	0.226	0.261	0.0538	1.37	1.5	0.71
0.7643	1.119	0.3568	0.223	0.258	0.0482	1.28	1.3	0.31
0.7989	1.107	0.3269	0.219	0.254	0.0441	1.17	1.1	0.41
0.8470	1.108	0.2981	0.214	0.248	0.0401	1.09	0.94	0.90
0.8934	1.118	0.2688	0.209	0.243	0.0374	0.986	0.82	0.76
0.9347	1.141	0.2405	0.206	0.239	0.0338	0.882	0.69	0.63
0.9871	1.176	0.2152	0.202	0.234	0.0301	0.807	0.59	0.88
1.0635	1.215	0.1915	0.196	0.227	0.0269	0.722	0.48	0.80

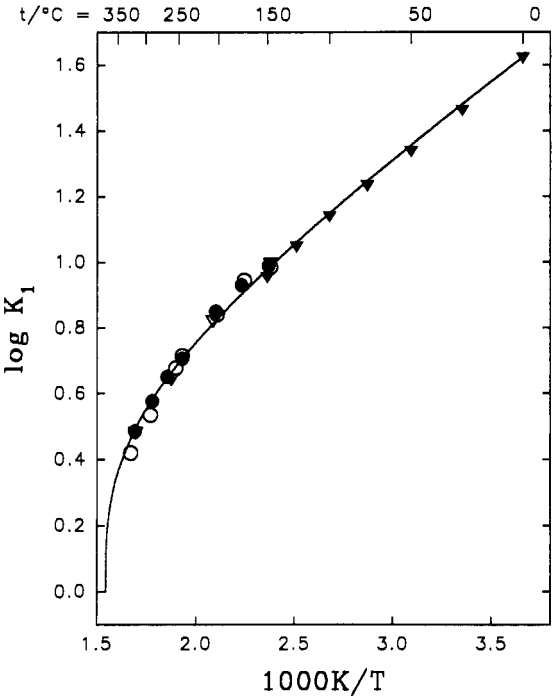

Figure 1. Liquid–vapor partitioning constant K_1 for NH_3: ○, ●, ▽, ref 10; ▼, ref 11. Solid curve calculated from eq 15.

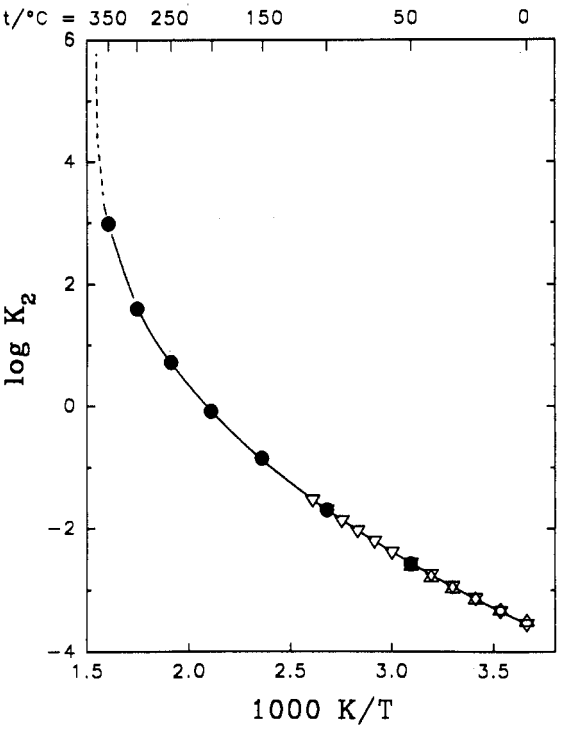

Figure 2. Liquid–vapor partitioning constant K_2 for HCl: ●, ref 12; ▽, ref 18; △, ref 19. Smooth curve calculated from eq 17.

$$\gamma_\pm^2(NH_4Cl) = \gamma_1(NH_4^+)\gamma_1(Cl^-) \quad (19)$$

Stoichiometric mean-ionic activity coefficients for hydrochloric acid have been determined from temperature integration of dilution enthalpy results to 375 °C coupled with measured values of activity coefficients at low temperatures. Holmes et al. (*8*) reported three models for the excess thermodynamic properties of HCl as functions of temperature, pressure, and molality which are applicable over selected ranges of experimental conditions. Activity and osmotic coefficients for HCl used in this work were taken from model I of Holmes et al. (*8*), which is a straightforward application of the Pitzer ion-interaction model for electrolyte thermodynamics (*20*) applicable from $0 \le m/(\text{mol·kg}^{-1}) \le 7$, $0 \le t/°C \le 250$, and $p_s \le p/\text{bar} \le 400$, where p_s is the saturation vapor pressure for water. At higher temperatures, excess thermodynamic properties were calculated from the AI model of Simonson et al. (*9*). This treatment, also based on the Pitzer

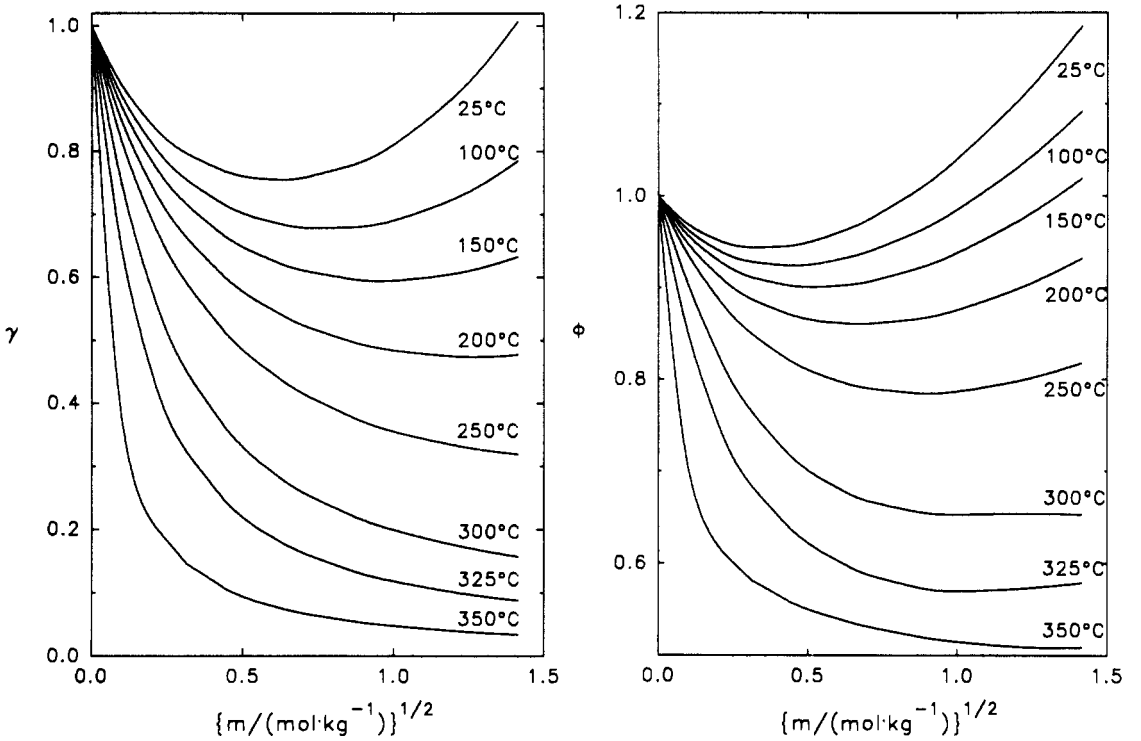

Figure 3. Activity and osmotic coefficients for HCl(aq) at the saturation vapor pressure. Values through 250 °C calculated from the equations of ref 8; values at higher temperatures from the equations of ref 9.

ion-interaction model, includes an explicit accounting for the ion association of HCl at high temperatures in the liquid phase through an extrapolation of the ion-pairing constants determined by Frantz and Marshall (*16*) from electrical conductance measurements at supercritical conditions. Activity coefficients calculated from this treatment are valid to 375 °C at pressures from saturation to 400 bar and at HCl molalities ranging up to 2 mol·kg^{-1}. These activity coefficients at 250 °C are in agreement within experimental error with those from model I of Holmes et al. (*8*); thus, there is no inconsistency in calculating excess thermodynamic properties using different treatments in different temperature ranges. Although the AI model of Simonson et al. (*9*) recognizes explicitly the formation of ion pairs in HCl in the liquid phase, activity coefficients reported in that work are given as stoichiometric quantities. Activity and osmotic coefficients for HCl(aq) at saturation vapor pressure are shown as functions of molality at various temperatures in Figure 3.

Enthalpies of dilution for NH_4Cl at molalities to 6 mol·kg^{-1} have been reported to 250 °C and at pressures to 350 bar by Thiessen and Simonson (*7*). Equations for activity and osmotic coefficients obtained by temperature integration of the dilution enthalpies with appropriate integration constants were also given (*7*). This representation for excess thermodynamic properties to 250 °C has been used to calculate values of activity and osmotic coefficients of NH_4Cl(aq) at the molalities of interest in this study. It was necessary to estimate these coefficients at temperatures above 250 °C. Plots of $\ln\{\gamma_\pm(NH_4Cl)/\gamma_\pm(NaCl)\}$ and $\phi(NH_4Cl) - \phi(NaCl)$ against temperature from 100 to 250 °C and at molalities ranging from 0.1 to 2 mol·kg^{-1} were found to be approximately linear over this temperature range, and were extrapolated linearly from 250 to 350 °C. Activity and osmotic coefficients for NH_4Cl(aq) were then calculated using these extrapolated differences and the corresponding quantities for NaCl(aq) from Pitzer, Peiper, and Busey (*21*) to 300 °C, and from Busey, Holmes, and Mesmer (*22*) at higher temperatures. This procedure introduces an uncertainty in the activity and osmotic coefficients for NH_4Cl(aq) which is difficult to estimate. Simonson (*23*) has noted that enthalpies of dilution of NH_4Cl(aq) at temperatures above 300 °C show a molality dependence which is not very different from that expected for a strong electrolyte at these temperatures due to a partial cancellation of the thermal effects of ammonium ion hydrolysis and ion-pair formation; thus, strong chemical effects on the stoichiometric activity coefficients of NH_4Cl(aq) are not expected. The difference between the extrapolated $\gamma_\pm(NH_4Cl)$ and $\gamma_\pm(NaCl)$ from Busey et al. (*22*) at 350 °C and 1 mol·kg^{-1} is about 15%. Assuming that the present estimation method gives a better value for $\gamma_\pm(NH_4Cl)$ than the model-substance approximation of $\gamma_\pm(NH_4Cl) \approx \gamma_\pm(NaCl)$, the uncertainty in the estimated activity coefficients should be on the order of a few percent. The estimated values of the activity coefficients $\gamma_\pm(NH_4Cl)$ and osmotic coefficients $\phi(NH_4Cl)$ at 300, 325, and 350 °C were fitted isothermally for the purpose of interpolation using the ion-interaction treatment of Pitzer with the additional ionic strength dependence in the second virial coefficient ($\beta^{(2)}$ term) (*24*) included to represent approximately the effects of ion association on the stoichiometric excess thermodynamic properties. Activity and osmotic coefficients for NH_4Cl(aq) at temperatures to 350 °C and molalities to 2 mol·kg^{-1} calculated by the methods described above are shown in Figure 4.

The activity and osmotic coefficients for NH_4Cl and HCl described above refer to stoichiometrically pure solutions. It is assumed here that the addition of ammonia has no effect on the activity or osmotic coefficients of ionic solutes (HCl or NH_4Cl) at the relatively low molalities of ammonia used in this work. The ion-interaction model is readily generalized to mixed electrolyte solutions. The stoichiometric mean-ionic activity coefficient of one component, MX, of a common-ion mixed electrolyte of 1–1 charge type may be written within the framework of the treatment as (*25*)

$$\ln \gamma_\pm(MX) = \ln \gamma_\pm^*(MX) + y[\phi^*(NX) - \phi^*(MX)] + my[\theta_{M,N} + (2-y)\psi_{M,N,X}/2] \quad (20)$$

where y is a cation molality fraction defined as $y = m_{NX}/$

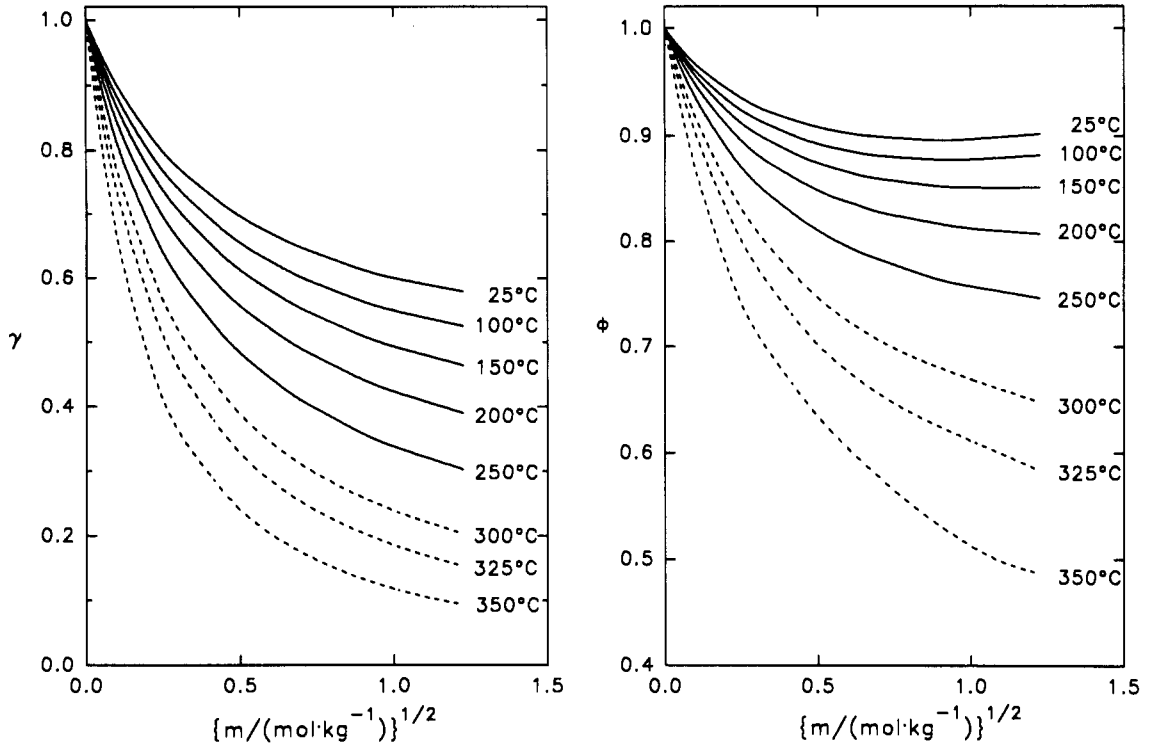

Figure 4. Activity and osmotic coefficients for NH_4Cl(aq) at the saturation vapor pressure. Values through 250 °C calculated from the equations of ref 7; values at higher temperatures estimated from NaCl values of refs 21 and 22 as described in the text.

($m_{MX} + m_{NX}$) and m is the total stoichiometric molality of solute in the mixture. Those marked with an asterisk are the pure-electrolyte quantities at the molality of the mixture, and the parameters $\theta_{M,N}$ and $\psi_{M,N,X}$ are mixture parameters describing the interactions between two cations, and between two cations and one anion, respectively. The activity coefficient for component NX is described by an expression corresponding to eq 20 with the component indices (MX and NX) exchanged. The mixing parameters $\theta_{M,N}$ and $\psi_{M,N,X}$ are not available at all temperatures of interest, and have been set equal to zero in calculating activity coefficients for these mixtures. Noting that these quantities are multiplied by the total stoichiometric molality of the mixed solution, this approximation should be reasonably good in cases where the total molality is not large, i.e., for the measurements at high temperatures. At the lower temperatures considered here it is expected that the values of the mixing parameters will be relatively small, and that errors on the order of a few percent in the activity coefficient may be introduced by neglecting these terms. The working equation for calculating activity coefficients of one component of a mixture reduces to

$$\ln \gamma_{\pm}(MX) = \ln \gamma_{\pm}^{*}(MX) + y[\phi^{*}(NX) - \phi^{*}(MX)] \quad (21)$$

Values of the partitioning constant K_3 for NH_4Cl were obtained from the experimental results listed in Tables I and II by difference methods. Expected levels of total nitrogen and total chloride in the vapor-phase samples were calculated from the known partitioning constants for NH_3 and HCl as given by eqs 11 and 12 and the parameters of eqs 15 and 17, using the stoichiometric activity coefficient of HCl appropriate for the mixture. Molalities of NH_4Cl in the vapor-phase samples were assumed to be equal to the difference between the observed chloride molality and that calculated from HCl partitioning, and equivalently by the difference between the observed total nitrogen molality and that calculated from NH_3 partitioning. These differences are often a small fraction of the total solute (either nitrogen or chloride) observed in the vapor-phase samples, leading to large overall uncertainties in the partitioning constants, particularly at low temperatures. For experiments conducted in excess acid (Table I) the low levels expected for ammonia should result in higher precision of the values of K_3 determined on the basis of the nitrogen analyses. Conversely, for runs over higher pH buffered solutions (Table II) the levels of chloride observed in the vapor phase should provide a more precise measure of ammonium chloride partitioning. Due to analytical difficulties in determining chloride molalities in vapor-phase samples in the presence of excess ammonia, and a somewhat larger uncertainty in ammonia analyses as compared with chloride determinations, in practice the values of K_3 determined on either basis include comparable uncertainties. In the most unfavorable cases, e.g., the measurements at 120 °C detailed in Table I, values of K_3 calculated on one basis gave physically-unreal negative values due to an excess of calculated over observed solute molalities in the vapor-phase samples.

A test of the applicability of the activity coefficients used in these calculations is provided by examining the series of measurements in a given experiment. Liquid-phase solute molalities tended to increase during each series due to removal of water from the liquid phase. If the molality dependence of the activity coefficients were significantly in error, the calculated values of K_3 would be expected to show a trend with the sample number (changing liquid-phase molality) within a given experiment. As shown in Figure 5 for the example case of K_3 calculated from excess chloride molality in the vapor-phase samples at 300 °C [Table I], the decrease in $\gamma_{\pm}^2$ for NH_4Cl compensates for the increasing liquid-phase molalities of ammonium and chloride, resulting in nearly constant calculated values of K_3. Thus, the values of K_3 discussed subsequently were obtained from averaging the values obtained by both difference methods for the multiple measurements of a given experiment.

The first vapor-phase sample in each series differed significantly from the remaining samples, so these were not used in calculating the average values of K_3. The values of $\log K_3$ and their associated uncertainties (3 times the standard

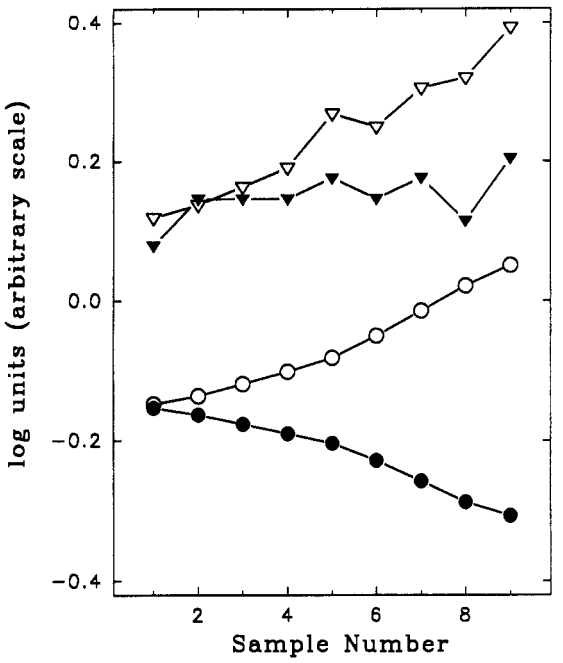

Figure 5. Measured and calculated quantities for experiments in excess HCl at 300 °C (Table I) illustrating the contributions of various terms to log K_3 calculated from excess vapor-phase nitrogen: ○, log m_l(Cl); ●, 2 log γ(NH_4Cl) − 1; ▽, log m_v(NH_3) + 2.5; ▼, log K_3(N) − 1.

Table III. Average Values and Uncertainties of log K_3

t/°C	exptl Nr[a]	log K_3[Cl][b]	3σ	log K_3[N][c]	3σ
125	A1			−6.34	1.13
150	A2			−4.72	0.88
150	A3	−3.55	0.57	−3.92	0.27
150	A4	−3.54	0.75	−3.40	0.59
150	A5			−4.29	0.50
200	A6	−2.82	0.41	−3.23	0.61
200	A7	−2.82	0.55	−3.19	0.90
200	A8	−3.22	0.50	−3.18	0.54
250	A9	−2.09	0.29	−2.35	0.36
300	A10	−0.85	0.06	−1.54	0.22
325	A11	1.11	0.23	1.20	0.23
325	A12	0.69	0.66	0.26	0.31
350	A13	1.57	0.33	1.53	0.33
350	A14	1.57	0.19	1.67	0.17
350	A15	1.78	0.34	1.77	0.41
200	A16	−3.60	0.57		
250	A17	−3.96	0.60	−0.03	0.33
300	A18	−0.04	0.31	−0.23	0.39

[a] Experimental results in Table I. [b] Calculated on the basis of excess chloride in vapor-phase samples. [c] Calculated on the basis of excess nitrogen in vapor-phase samples.

error of the mean) are presented in Table III. The tabulated uncertainty in the averaged values of log K_3 has been taken to be $\delta \log K_3 = \log(K_3 + 3\sigma) - \log K_3$. The averaged experimental values of log K_3 are plotted against reciprocal temperature in kelvin in Figure 6. The solid lines in this figure are smoothed values calculated from two different fitting equations:

$$\log K_3 = -1.875 - 1248.65/(T/\mathrm{K}) - 23.401 \log(\rho_l/(\mathrm{g\cdot cm^{-3}})) \quad (22)$$

$$\log K_3 = -16.063 + 15203.4/(T/\mathrm{K}) - 9.3301 \log(\rho_l/\rho_v) \quad (23)$$

It is clear from inspection of Figure 6 that either eq 22 or 23 provides an equally good representation of the experimental results. The difference between the two fitting equations

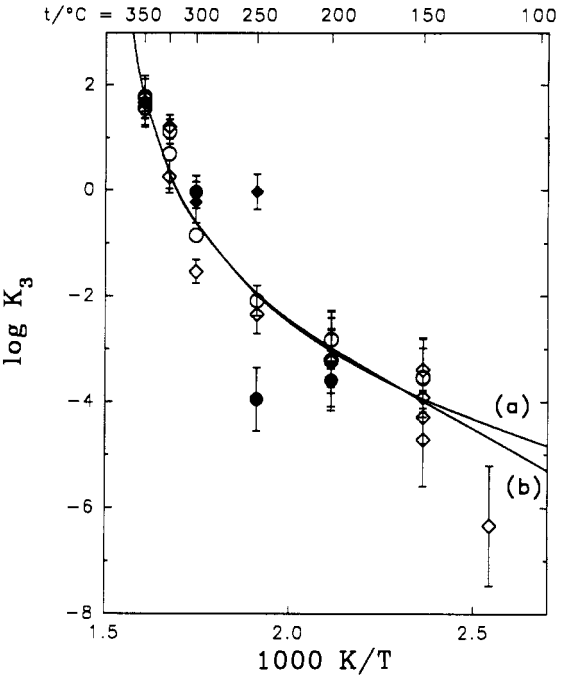

Figure 6. Liquid–vapor partitioning constant K_3 for NH_4Cl: ○, excess chloride basis, excess acid measurements; ◇, excess nitrogen basis, excess acid measurements; ●, excess chloride basis, buffered measurements; ◆, excess nitrogen basis, buffered measurements. Curve a calculated from eq 22; curve b calculated from eq 23.

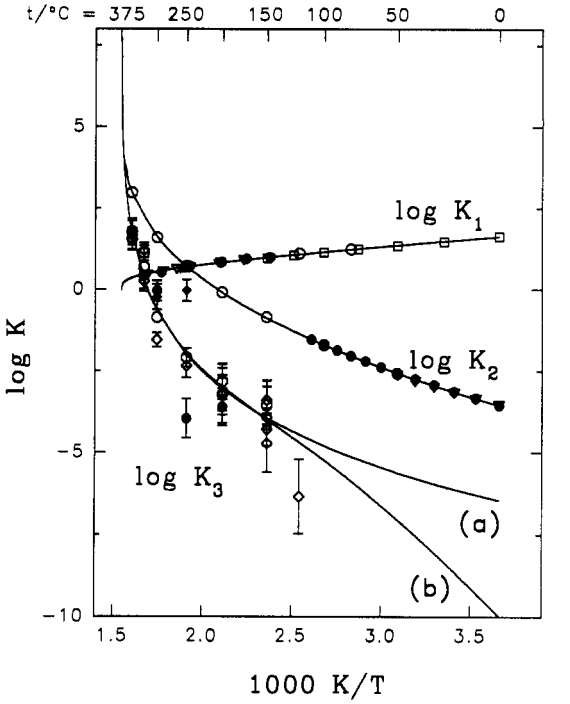

Figure 7. Comparison of liquid–vapor partitioning constants for NH_3, HCl, and NH_4Cl.

lies in the extrapolation to temperatures lower than those at which values of K_3 could be determined experimentally. The two functions give extrapolated values which differ by about 3 log units at 25 °C.

The three liquid–vapor partitioning constants K_1, K_2, and K_3 for NH_3, HCl, and NH_4Cl are plotted against reciprocal temperature in kelvin in Figure 7 where curves generated from eqs 15, 17, and 22 are shown as solid lines; all three curves are shown extrapolated to the solvent critical temperature (374 °C) (*26*). The curve representing the parti-

tioning constant of the neutral molecule NH_3 extrapolates to $\log K_1 = 0$ at $t = t_c$; indeed, this criterion was adopted as a fitting condition in determining the parameters of eq 15. The two expressions describing the partitioning constants for HCl and NH_4Cl clearly do not extrapolate to $\log K_2 = \log K_3 = 0$ at $t = t_c$. This is due to the fact that the basis adopted for the representation of partitioning coefficients is the equilibrium between stoichiometric total solutes in the liquid phase and associated molecular solutes in the vapor phase. This basis, which is thermodynamically rigorous within the assumption that the neutral molecules in the vapor phase have unit activity coefficients, has been adopted in order to make use of the available stoichiometric liquid-phase activity coefficients for HCl and NH_4Cl. This representation has the additional advantage of removing the requirement of estimating liquid-phase association constants for these solutes under conditions where these constants are small and hence ambiguous. On a stoichiometric basis, the partitioning constants K_2 and K_3 extrapolate to the values of the liquid-phase ion association constant at the critical temperature. For example, for the case of HCl, the association equilibrium constant for eq 4 is given by

$$K_a = \frac{m_l(\mathrm{HCl})}{m_l(\mathrm{H^+})m_l(\mathrm{Cl^-})\gamma_\pm^2(\mathrm{HCl})} \quad (24)$$

such that

$$K_2 = \frac{m_v(\mathrm{HCl})}{m_l(\mathrm{H^+})m_l(\mathrm{Cl^-})\gamma_\pm^2(\mathrm{HCl})} = \frac{m_v(\mathrm{HCl})}{m_l(\mathrm{HCl})}K_a = K_v K_a \quad (25)$$

where K_v is the real partitioning coefficient for HCl as defined by eq 7. Thus, it is of interest to compare the extrapolated partitioning constants of electrolytes at the critical temperature with the corresponding results obtained from extrapolation of higher temperature electrical conductance measurements (*14*, *15*). For HCl, eq 17 extrapolates to $\log K_2 = 5.89$ at t_c, as compared with an extrapolated value for the association constant of HCl (eq 4) of $\log K_a(\mathrm{HCl}) = 6.27$ (*15*). This level of agreement is very good considering the relatively long extrapolations in temperature and density required for both the conductance and partitioning results. For NH_4Cl, eqs 22 and 23 extrapolate to comparable values of $\log K_3 = 7.71$ and 7.43, respectively, at t_c. These values seem somewhat larger than might be expected for $\log K_a(NH_4Cl)$ (eq 3) on the basis of reduced charge density on the ammonium ion as compared with hydrogen or sodium ion. The value of $\log K_a(\mathrm{NaCl}) = 3.78$ at t_c is calculated from fitting the conductance data of Quist and Marshall (*14*) to the form of eq 22. However, this value is at least qualitatively comparable to those for the other electrolytes studied, and a possible added contribution to the stability of the NH_4Cl ion pair from hydrogen bonding cannot be ruled out. Given the limited precision of the partitioning constants for NH_4Cl, the relatively long extrapolation (more than 5 log units) of eqs 22 and 23 from 350 °C to t_c, the uncertainty in activity coefficients of HCl and NH_4Cl in mixtures at high temperatures, and the lack of a sound theoretical basis for prediction of association constants of NH_4Cl at the solvent critical conditions, there is no reason to assume that the partitioning constants calculated from these experiments are unreasonable on the basis of this extrapolation to the solvent critical conditions.

Application to Power Plant Operating Conditions

For the particular question of transport of chloride in steam generators using AVT to control pH, it is important to note that this study shows that under high-temperature conditions the relative magnitudes of the partitioning constants of NH_4Cl, NH_3, and HCl (given in Table IV at selected temperatures) are such that at low ammonium ion molalities the major source of chloride in the vapor phase is the partitioning of HCl from the liquid. At 350 °C the hydrogen ion molality in pure water, taken from the representation of the ion product of Marshall and Franck (*4*), is about 7×10^{-7} mol·kg^{-1}, while the difference between the values of $\log K_2$ and $\log K_3$ is about 1.25. Thus, for a given chloride molality, a stoichiometric ammonium molality of about 1.2×10^{-5} mol·kg^{-1}, corresponding to about 0.2 ppm ammonium, is required to partition chloride to the vapor phase equally as HCl and NH_4Cl. Clearly under the usual AVT conditions with ammonium ion levels of tens of parts per billion and high-temperature pH values near neutral, transport of chloride ion to the vapor phase as HCl will dominate transport as NH_4Cl. It can be seen from inspection of Figure 7 that this situation is even more prevalent at lower temperatures, because the difference between $\log K_2$ and $\log K_3$ increases with decreasing temperature.

Table IV. Equilibrium Constants Relevant to Partitioning Calculations

t	$\log K_1$	$\log K_2$	$\log K_3$	$\log K_H$	$\log K_W$
350	0.36	2.98	1.76	−4.30	−12.30
300	0.55	1.62	−0.63	−4.70	−11.41
275	0.62	1.14	−1.35	−4.93	−11.25
195	0.84	−0.18	−3.08	−5.85	−11.31
150	0.98	−0.88	−3.99	−6.51	−11.64
100	1.15	−1.69	−5.22	−7.40	−12.26

The primary contribution of HCl partitioning to the chloride content in the vapor phase does not imply that the subsequent deposition of chloride in the early condensate in the water/steam cycle will be as HCl. Under equilibrium conditions, and assuming no dry deposition of solutes from superheated steam or reaction of the solutes in steam with solid phases or metal surfaces, the primary vector for enhancement of chloride in the early condensate is the steep decrease in the partitioning constant for NH_4Cl with decreasing temperature. The product of chloride and ammonium molalities in the condensate will increase by approximately 1 order of magnitude as compared with the corresponding molality product in the boiling liquid phase for each log unit decrease in K_3 resulting from the decrease in temperature between boiling and condensation.

Approximate calculations based on the partitioning coefficients discussed here were carried out to simulate field monitoring analytical studies (*1*, *2*) at a number of utilities (*27*). Although more experimental and detailed monitoring data are needed for a rigorous comparison of such results, including detailed charge-balance considerations in both phases within the power plant water/steam cycle, correlations of this kind provide the opportunity for a better understanding and subsequent control of the water chemistry in power plants.

Summary

The partitioning coefficient of ammonium chloride between aqueous liquid and vapor phases has been measured experimentally for the first time. These measurements were conducted from 120 to 350 °C by analyzing samples of both phases. The volatilities of HCl, NH_3, and NH_4Cl were considered in the analyses and data reduction, with the volatilities of HCl and/or NH_3 exceeding that of NH_4Cl in all experiments. Available, experimentally-determined activity coefficients for all the ionic species involved allowed consistent and reasonable extrapolation of the partitioning coefficients measured at relatively high concentrations in the laboratory to dilute conditions encountered in power-generating cycles. A simple three-term equation describes the temperature dependence of the logarithm of the partitioning constant of NH_4Cl over the measured temperature range. Knowledge of

the partitioning constants for HCl, NH_3, and NH_4Cl, as well as of the hydrolysis constant for NH_3, as functions of temperature permits calculation of the speciation between these species and their ionized forms during transport via the steam phase from boiler water to formation of early condensate. Under the conditions simulated in speciation calculations, the dominant chloride species in the steam phase is HCl, and although the dominant cation (ignoring as yet unknown effects of other cations such as Na^+) in the early condensate is NH_4^+, this solution is considerably more acidic than the boiler water. The ray diagram as presently used is unsuitable either for predicting the levels of solutes expected in steam or for assigning the compound primarily responsible for liquid–vapor partitioning, because the dependence of the partitioning on liquid-phase concentrations of both cations and anions is not recognized.

Acknowledgment

The authors are pleased to acknowledge extensive discussions with Robert E. Mesmer, Chemistry Division, ORNL. The guidance of R. B. Dooley (Electric Power Research Institute) and O. Jonas (Jonas, Inc.) in all matters related to the application to power generation technology is gratefully acknowledged.

Literature Cited

(1) Aschoff, A. F.; Sopocy, D. M.; Eglar, D. T. Monitoring Cycle Water Chemistry in Fossil Plants. Volume 1: Monitoring Results. EPRI Report GS-7556; Electric Power Research Institute: Palo Alto, CA, 1987.
(2) Aschoff, A. F.; Sopocy, D. M.; Eglar, D. T. Monitoring Cycle Water Chemistry in Fossil Plants. Volume 3: Project Conclusions and Recommendations. EPRI Report GS-7556; Electric Power Research Institute: Palo Alto, CA, 1991.
(3) Martynova, O. I. In *High Temperature High Pressure Electrochemistry in Aqueous Solutions*; Staehle, R. W., Jones, D. de G., Slater, J. E., Eds.; International Corrosion Conference Series NACE-4; National Association of Corrosion Engineers: Houston, TX, 1976; pp 131–138.
(4) Marshall, W. L.; Franck, E. U. An Equation for the Ion Product of Water: 0–1000°C, 1–10,000 Bars. In *Water and Steam. Their Properties and Current Industrial Applications*; Straub, J., Scheffler, K., Eds.; Pergamon Press; New York, 1980; p 806.
(5) Quist, A. S.; Marshall, W. L. *J. Phys. Chem.* **1968**, *72*, 3122.
(6) Hitch, B. F.; Mesmer, R. E. *J. Solution Chem.* **1976**, *5*, 667.
(7) Thiessen, W. E.; Simonson, J. M. *J. Phys. Chem.* **1990**, *94*, 7794.
(8) Holmes, H. F.; Busey, R. H.; Simonson, J. M.; Mesmer, R. E.; Archer, D. G.; Wood, R. H. *J. Chem. Thermodyn.* **1987**, *19*, 863.
(9) Simonson, J. M.; Holmes, H. F.; Busey, R. H.; Mesmer, R. E.; Archer, D. G.; Wood, R. H. *J. Phys. Chem.* **1990**, *94*, 7675.
(10) Jones, M. E. *J. Phys. Chem.* **1963**, *67*, 1113.
(11) Edwards, T. J.; Maurer, G.; Newman, J.; Prausnitz, J. M. *AIChE J.* **1978**, *24*, 966.
(12) Simonson, J. M.; Palmer, D. A. *Geochim. Cosmochim. Acta* **1993**, *57*, 1.
(13) Marshall, W. L.; Mesmer, R. E. *J. Solution Chem.* **1981**, *10*, 121.
(14) Marshall, W. L.; Mesmer, R. E. *J. Solution Chem.* **1984**, *13*, 383.
(15) Quist, A. S.; Marshall, W. L. *J. Phys. Chem.* **1968**, *72*, 684.
(16) Frantz, J. D.; Marshall, W. L. *Am. J. Sci.* **1984**, *284*, 651.
(17) Haar, L.; Gallagher, J. S.; Kell, G. S. *NBS/NRC Steam Tables. Thermodynamic and Transport Properties and Computer Programs for Vapor and Liquid States of Water in SI Units*; Hemisphere Publishing Corp.: New York, 1984; pp 9–15.
(18) *International Critical Tables*; McGraw-Hill: New York, 1928; Vol. III, p 501.
(19) Fritz, J. J.; Fuget, C. R. *Ind. Eng. Chem.* **1956**, *1*, 10.
(20) Pitzer, K. S. *J. Phys. Chem.* **1973**, *77*, 268.
(21) Pitzer, K. S.; Peiper, J. C.; Busey, R. H. *J. Phys. Chem. Ref. Data* **1984**, *13*, 1.
(22) Busey, R. H.; Holmes, H. F.; Mesmer, R. E. *J. Chem. Thermodyn.* **1984**, *16*, 343.
(23) Simonson, J. M. Chemistry Division Annual Progress Report for Period Ending March 1, 1991. ORNL-6668; Oak Ridge National Laboratory: Oak Ridge, TN, 1991; pp 28, 29.
(24) Pitzer, K. S.; Mayorga, G. *J. Solution Chem.* **1974**, *3*, 539.
(25) Holmes, H. F.; Mesmer, R. E. *J. Chem. Thermodyn.* **1988**, *20*, 1049.
(26) Levelt Sengers, J. M. H.; Straub, J.; Watanabe, K.; Hill, P. G. *J. Phys. Chem. Ref. Data* **1985**, *14*, 193.
(27) Palmer, D. A.; Simonson, J. M. Experimental Studies of the Volatility of Ammonium Chloride. EPRI Report; Electric Power Research Institute: Palo Alto, CA, in press.

Received for review March 9, 1993. Accepted April 21, 1993. Financial support for this project was provided by the Electric Power Research Institute under Contract Number DE-AC05-84OR21400 with Martin Marietta Energy Systems, Inc.